Cement and Concrete Research 42 (2012) 633–641

Contents lists available at SciVerse ScienceDirect

Cement and Concrete Research

journal homepage: http://ees.elsevier.com/CEMCON/default.asp

Flow induced particle migration in fresh concrete: Theoretical frame, numerical simulations and experimental results on model fluids

J. Spangenberg [a], N. Roussel [b,*], J.H. Hattel [a], H. Stang [c], J. Skocek [c], M.R. Geiker [c,d]

[a] Department of Mechanical Engineering, Technical University of Denmark (DTU), Denmark
[b] Université Paris Est, Laboratoire Central des Ponts et Chaussées (LCPC), France
[c] Department of Civil Engineering, Technical University of Denmark (DTU), Denmark
[d] Department of Structural Engineering, Norwegian University of Science and Technology, Norway

ARTICLE INFO

Article history:
Received 15 November 2011
Accepted 31 January 2012

Keywords:
Fresh concrete (A)
Rheology (A)
Aggregate (D)
Modelling (E)
Segregation

ABSTRACT

In this paper, we describe and compare the various physical phenomena which potentially lead to flow induced particle migration in concrete. We show that, in the case of industrial casting of concrete, gravity induced particle migration dominates all other potential sources of heterogeneities induced by flow. We then show, from comparisons between experiments using model materials, dimensional analysis and numerical simulations, that, from a quantitative point of view, the viscous drag force, which prevents particles from migrating during a casting process, shall neither be computed from the apparent viscosity nor from the plastic viscosity of the suspending phase but from its tangential viscosity. Finally, the transfer of this type of numerical prediction tool to real concrete is discussed.

1. Introduction

At the scale of a structural element such as a beam or a slab, concrete is a heterogeneous material. This is even more so the case if constitutive aggregates get segregated during the flow induced by casting processes or if they settle when concrete is at rest before setting.

In the traditional industrial description of self compacting concrete property requirements, the so-called "resistance to dynamic segregation" is often distinguished from the "resistance to static segregation". The first one is associated with flow induced particle migration originating from various phenomena whereas the second one is only associated with the aggregate settling process due to the density difference between the components when the material is at rest before or after casting.

Static segregation has been the topic of several papers [1–4]. These papers either deal with the measurement or the prediction of this phenomenon. They show that yield stress and thixotropy seem to dictate static segregation for a given granular skeleton.

Dynamic segregation (i.e. flow induced particle migration) has however been far less studied. Depending on the considered concrete flow, different phenomena can dominate and dictate particle migration within the material.

In this paper, we first describe and compare the various physical phenomena which potentially lead to flow induced particle migration. We compare their influence on the local aggregates volume fraction to the geometrically induced particle heterogeneity due to wall effect. We show for instance that shear induced particle migration and wall effect dominate in pumping processes whereas, in the case of industrial casting of concrete, gravity induced heterogeneity dominates over all other potential sources of heterogeneities induced by flow.

In the second part, we compare experimental measurements of flow induced particle migration, dimensional analysis and numerical simulations. We conclude on the value of the viscosity that has to be considered when studying particle migration during a casting process.

Moreover, based on the aforementioned results, it is found that it is possible to numerically predict gravity induced particle migration in the case of the casting of a model material, designed to mimic self compacting concrete.

Finally, the transfer of this type of numerical prediction tool to real concrete is discussed.

2. Flow induced particle migration

In this section, the consequences of the physical phenomena at the origin of flow induced particle migration on local aggregates volume fraction are compared. Although we do not deal with detailed processing problems, we provide here general orders of magnitude. Three main types of flow induced particle migration are identified:

- Shear induced particle migration
- Gravity induced particle migration
- Granular blocking

* Corresponding author at: IFSTTAR, 158, Bd. Lefebvre, 75732 Paris Cedex 15, France. Tel. +33 140435285.

0008-8846/$ – see front matter © 2012 Elsevier Ltd. All rights reserved.
doi:10.1016/j.cemconres.2012.01.007

For each particle migration phenomenon, the maximum induced local particle volume fraction variation and the characteristic time of this migration are estimated. Then, in order to estimate the global effect at the scale of the concrete flow, we ponder the local volume fraction variation by the size of the zone where the particle migration is expected to occur. We moreover compare the consequences of the above phenomena with particle heterogeneity induced by the wall effect.

2.1. Flow description

In the types of flow considered here, the smallest dimension will be denoted the thickness H. The flows can be industrial casting processes (the thickness is then the smallest dimension of the element to be cast), pumping flows (the thickness is then the radius of the pipe) or flows within rheometers or acceptance tests such as slump or slump flow test. The characteristic flow time is denoted T_f. In the case of a transient flow, this could be, for instance, the duration of the flow from flow start to stop. In the case of a steady state flow such as pumping, it could be the time spent by the concrete in the pumping pipe. The flow characteristic length (i.e. the propagation length in transient flows or the largest flow dimension in steady state flows) is denoted L. In the case of casting, this could, for instance, correspond to the length or the half length of a beam depending on the casting process. In the case of pumping, this could correspond to the length of the pipe. In these flows, the material flows at an average velocity V and is subjected to an average shear rate $\dot{\gamma}$. The quantities $\dot{\gamma}$, V,L, H and T_f are linked through the following dimensional relations: $T_f = L/V$ and $\dot{\gamma} = V/H$.

2.2. Shear induced particle migration

Particle collisions in highly sheared and/or highly concentrated zones force particles to migrate from these zones. This effect is counterbalanced by the local increase in the suspension viscosity resulting from this migration. Shear induced particle migration finds therefore its origin in the competition between gradients in particle collision frequency and gradients in viscosity of the suspension.

Leighton and Acrivos [5] and Phillips et al. [6] modeled the complex diffusion process associated with shear induced particle migration. The diffusion coefficient D may be written as $D \cong \bar{D}(\phi)\dot{\gamma}a^2$ [7,8] where ϕ is the solid volume fraction, $\dot{\gamma}$ the shear rate, a the size of the particles and $\bar{D}(\phi)$ a dimensionless diffusion coefficient proportional to the power two of the volume fraction $\bar{D}(\phi) \propto \phi^2$ [9]. Note here the power two of the particle diameter appearing in the value of the diffusion coefficient showing that coarse particles are the most prone to shear induced migration.

Shear induced particle migration is often strongly localized in highly sheared zones at interfaces. It can therefore strongly affect flow by creating lubricating layers such as the ones observed during concrete pumping processes [10–13] or during rheometric testing on concrete or mortars [14]. Recent and detailed numerical simulations of shear induced particle migration were carried out in the case of pumping [15]. The results showed that shear induced particle migration is indeed inducing the slippage layer of several mm at the interface between the material and the pipe during pumping processes. In this zone, not only the coarsest particles are migrating but also sand grains.

Shear induced particle migration reaches equilibrium because of the increase in viscosity of the zones where particles are migrating to. It can then be expected that shear induced migration shall stop before the local particle volume fraction is high enough to reach the so-called random loose packing (i.e. the lowest volume fraction value allowing for a percolated network of contacts between particles). It was shown recently that this random loose packing can be estimated from the value of the maximum packing fraction ϕ_m of the particles and is of the order of $0.8\phi_m$ [16–18].

As a consequence, it can be expected that the highest variation in particle volume fraction due to shear induced particle migration after an infinite time shall be lower than:

$$\Delta\phi^{shear} = \phi_0\left(1 - \frac{\phi_0}{0.8\phi_m}\right) \tag{1}$$

where ϕ_0 is the mix design particle volume fraction.

Let us now consider the characteristic time associated to shear induced particle migration. Most experimental studies show that the particle volume fraction profile reaches a steady state after a certain critical deformation γ_c of the suspension [6,9,19–21]. Recent results [9] have however shown, using MRI measurements, that, in the case of concentrated suspensions, this critical deformation seems to be one order of magnitude lower than expected. This peculiar effect was attributed to a local shear thickening of the material, which enhances particle migration [9]. It can be estimated from the above studies that the critical deformation, above which steady state is reached, in the case of concrete or mortars shall be of the order of $\gamma_c \cong H^2/10a^2\phi^2$. Shear induced particle migration shall therefore reach its full extent after a characteristic shear induced particle migration time T_c^{shear} of the order of:

$$T_c^{shear} = \frac{H^2}{10a^2\phi^2\dot{\gamma}}. \tag{2}$$

2.3. Gravity induced particle migration

We will only deal here with the case of materials which are stable at rest [1,2] and focus on the particle migration induced by gravity when concrete is flowing and/or being cast [22]. It can however be reminded here that, in order to produce a concrete, which stays homogeneous at rest, the constitutive cement paste or mortar must either have a sufficient yield stress [1,2,23] or sufficient thixotropic structuration rate to quickly build up a structure able to support the coarsest particles [24,25].

When the material flows, the stress generated by gravity in the mixture is higher than the yield stress of the material. This means that any additional stress, such as the one generated by a density difference between an aggregate and the surrounding mixture, could induce a local flow around the aggregate even if this additional stress itself is lower than the yield stress.

Gravity induced particle migration during casting results therefore from the competition between the difference in density of the mixture components that force them to separate and the viscous drag of the flowing suspending fluid that slows down the phenomenon. Contrarily to shear induced particle migration, it is not a diffusion process but an advection process. The force induced by the density difference can be written as $F_{gravity} = g\Delta\rho\pi a^3/6$, where $\Delta\rho$ is the density difference between the aggregates and the suspending phase. Viscous drag can be computed, as a first approximation, from Stoke's law for dilute spheres in Newtonian fluids, $F_{viscous} = 3\pi\mu_0 a V_s$, where μ_0 is the viscosity of the suspending phase and V_s is the relative settling velocity of the aggregate in the suspending fluid. This relative velocity, in the case of aggregates heavier than the suspending fluid is a vertical settling velocity and can be written as $V_s = g\Delta\rho a^2/18\mu_0$. This approach neglects any effect of the yield stress of the surrounding fluid. It also neglects any other non Newtonian features. This aspect will however be discussed further in this paper.

As in the previous section, it can be expected that gravity induced particle migration shall stop before the local particle volume fraction reaches the so-called random loose packing. As a consequence, the highest variation in particle volume fraction due to gravity induced

particle migration is the same as the one due to shear induced particle migration:

$$\Delta\phi^{gravity} = \Delta\phi^{shear} = \phi_0\left(1-\frac{\phi_0}{0.8\phi_m}\right) \quad (3)$$

The characteristic time associated to this process is however very different. Being an advection process, it can be estimated as:

$$T_c^{gravity} \cong \frac{H}{V_s} = \frac{18\mu_0 H}{g\Delta\rho a^2}. \quad (4)$$

It is worth noting that the coarsest aggregates are once again most prone to a fast migration because of the power two of the particle diameter appearing in Eq. (4).

2.4. Granular blocking induced heterogeneities

We will not deal much here with this type of flow induced heterogeneity as we assume that, in proper industrial castings with properly mix designed materials, the size of the coarsest particles is compatible with the gap between reinforcement bars within the element to be cast [26–30] or with the thickness of the flow.

It should also be kept in mind here that the granular blocking phenomenon is of a probabilistic nature. The probability of granular blocking increases with the number of particles crossing the obstacles, their volume fraction and the ratio between the diameter of the particles and the gap between the obstacles. As long as it is not coupled with another source of flow induced particle migration, which could increase the local particle volume fraction at the vicinity of the obstacles, this phenomenon seems to only depend on geometrical considerations and not depend on the rheology of the suspending fluid.

Finally, it shall be kept in mind that this type of particle migration shall dominate all others when they occur as they are able to concentrate particle up to and above the loose packing fraction in the vicinity of the obstacles. They may also prevent the proper filling of the formwork [31–33].

2.5. Heterogeneity in particle distribution induced by the wall effect

Variations in local particle volume fraction may also be induced by the presence of walls. This phenomenon is not induced by flow but, because of simple geometrical considerations, it is not possible to find the center of a particle of diameter a at a distance from a wall lower than $a/2$ [34]. Because of this wall effect, there exists therefore some heterogeneity at the vicinity of any solid interface within the flow.

Thus, in a plane parallel to the wall, the coarse particle volume fraction will be the sum of contributions from all coarse particles with centers within $a/2$ of the plane. If the plane is at a short distance δ from the wall compared to the size of the particles, the particle volume fraction at the plane is small since there are relatively few particles with centers within a distance $a/2$ of the plane (only those with centers between $a/2$ and $a/2+\delta$ can contribute). As the plane is moved further from the wall, more and more particles can contribute to the coarse particle volume fraction. The coarse particle volume fraction therefore increases from the wall. At a distance a, none of the suspension within $a/2$ of the considered plane is devoid of coarse particle centers. The coarse particle volume fraction reaches then its bulk value. The coarse particle volume fraction increases therefore from zero at the wall to the bulk volume fraction at a distance a. Its average value in the depleted zone can be estimated as half the bulk volume fraction $\phi_0/2$.

This phenomenon however only concerns interface zones, the characteristic thickness of which is, as shown above, of the order of a and therefore smaller than the characteristic size of the concrete element to be cast. At the scale of the concrete flow of thickness H, the variation in coarse particle volume fraction due to wall effect shall therefore only be of the order:

$$\Delta\phi^{walleffect} \cong \frac{\phi_0 a}{2H}. \quad (5)$$

2.6. Induced heterogeneities during concrete casting or testing

As it was shown in the previous sections, most particle volume fraction variations induced by flow are increasing functions of the diameter of the particles and are therefore stronger at the scale of the coarsest aggregates. We choose here to focus on this fraction of the granular skeleton. As concrete contains in average 60 to 80% aggregates and as at least half of them by volume are coarse aggregates, we will therefore focus in the following on particles with a diameter of the order of 1 cm and a mix design volume fraction of approximately 40%.

We consider here the case (i) of the slump test for conventional concretes, (ii) of the slump flow test for self compacting concretes, (iii) of a typical concrete rheometer test and (iv) of typical casting and pumping processes. The quantities ϕ_0, a and $\Delta\rho$ are respectively considered as being around 40%, 0.01 m and 500 kg/m^3. The considered values for T, H, L and V are gathered in Table 1.

The typical value of the viscosity of the so-called suspending fluid is far more delicate to identify. The orders of magnitude of viscosities of cementitious suspensions at typical industrial shear rates are 0.1–1 Pa s for cement pastes, 1–10 Pa s for mortars and 10–100 Pa s for concretes [18,35]. If we consider that the suspending phase for the coarsest aggregates shall locate somewhere between the mortar scale and the concrete scale itself, we can consider $\mu_0 = 10$ Pa s as an order of magnitude.

In Table 2, the expected variations in coarse aggregates volume fraction are computed by considering that the fastest phenomenon (i.e. the one with the shortest characteristic time) occurs first. Its magnitude is proportional (and also limited) to the maximum particle volume concentration variation induced by this phenomenon and also proportional to the ratio between the duration of the flow and the characteristic time of the phenomenon. In the case of heterogeneities induced by the wall effect, we, of course, consider that it is instantaneous and occurs prior to other induced particle migration.

It can be concluded from Table 2 that, although shear induced particle migration and wall effect dominate during pumping processes, gravity induced particle migration dominates during typical industrial concrete casting processes.

The results in Table 2 moreover show that, although slump in the case of conventional concrete is only weakly affected by flow induced particle migration, slump flow for self compacting concrete is affected by both a potential gravity induced particle migration and wall effects. Because of these effects, there is no generally applicable correlation (i.e. independent of the concrete tested) between the slump flow value and yield stress as shown in [36].

Finally, the results in Table 2 show that shear induced and gravity induced particle migration shall affect the results obtained with

Table 1
Parameters describing typical concrete flows and the model casting studied in this paper.

Flow	L (m)	T_f (s)	H (m)	V (m/s)
Slump	0.2	2	0.15	0.1
Slump flow	0.4	4	0.05	0.1
Rheometer	–	60	0.1	0.5
Casting	5	50	0.2	0.1
Pumping	100	100	0.05	1
Model casting	0.6	90	0.055	0.007

Table 2
Origins and magnitude of average particles volume fraction variations due to flow induced particles migration in typical concrete flows and in the model casting studied in this paper.

Flow	Shear induced heterogeneities	Gravity induced heterogeneities	Wall effect induced heterogeneities
Slump	Neglectable	Neglectable	1–2%
Slump flow	Of the order of 1%	Of the order of 1%	3–5%
Rheometer	3–5%	1–2%	1–2%
Casting	Neglectable	5–10%	Of the order of 1%
Pumping	3–5%	Neglectable	3–5%
Model casting (beads diameter = 2 mm)	Neglectable	1%	Neglectable
Model casting (beads diameter = 5 mm)	Neglectable	5%	Neglectable
Model casting (beads diameter = 7 mm)	Neglectable	7%	Of the order of 1%

concrete rheometers. These phenomena, which depend on the exact geometry of the rheometer, may be at the origin of the discrepancy between the available concrete rheometers [37,38] as shown by recent MRI measurements on model mortars [14].

3. Experimental measurements

We have shown, in the previous section, that gravity induced particle migration dominates during typical industrial concrete casting processes. In order to reproduce this phenomenon in the laboratory, a combination of a model material and a model formwork able to mimic the casting of self compacting concrete is developed in this section.

3.1. Materials

We prepare our model concrete with a polymer gel and glass beads at a volume fraction of 10%, which aims at mimicking the behavior of a fluid (but transparent) concrete [39].

The polymer used in this work is Carbopol Ultrez (manufacturer Noveon), a transparent material that disperses faster than other conventional grades. Carbopol is used here at a volume fraction of 0.3%.

The dehydrated Carbopol powder is first slowly added to distilled water through a fine metal mesh using a variable speed mixer. The solution is then neutralized by a sodium hydroxide solution at 18%. A mixing period of 6 h follows this neutralization phase. Finally, the products are conserved at 25 °C for 2 days. The prepared carbopol suspension can then be diluted in distilled water in order to produce mixtures with yield stresses between 15 and 125 Pa. Before use, air bubbles are removed by a slow manual shearing. Because of the low polymer concentration, the density of the carbopol gel is very close to the density of water.

The Carbopol suspension used in this study is not thixotropic as shown by the superposition of measurements obtained for increasing and decreasing shear rate ramps in Fig. 1. We use a HAAKE ViscoTester VT550 equipped with coaxial cylinders, the inner cylinder of diameter 18.9 mm being in rotation whereas the outer cylinder of diameter 20.5 mm remains fixed. Both surfaces of the cylinders are covered with sand paper in order to avoid wall slip. The modified gap width is identified using a reference Newtonian oil. The behavior of the carbopol gel can either be fitted with a Bingham model ($\tau = \tau_0 + \mu_p \dot{\gamma}$) mixture with a yield stress τ_0 of 40 Pa and a plastic viscosity μ_p of 1 Pa s or fitted with a Herschel Bulkley model ($\tau = \tau_0 + K\dot{\gamma}^n$) with a yield stress τ_0 of 40 Pa, $K = 15.8$ Pa s and $n = 0.48$.

The Bingham model parameters for the carbopol alone are used further in this work for the prediction of the global flow of the glass beads and carbopol mixture in the model formwork. Because of the low volume fraction of the glass beads, the behavior of the glass beads and carbopol mixture does not strongly differ from the rheological behavior of the carbopol alone. It can indeed be expected from the theoretical work of Chateau et al. [40,41] that the yield stress of the mixture shall be around 1.09 times the yield stress of the carbopol whereas its plastic viscosity shall be around 1.3 times the plastic viscosity of the carbopol. Because of these low fluctuations of the rheological parameters with the local concentration of glass beads, the influence of flow induced heterogeneities on local rheological properties and on the global flow of the mixture will be neglected in the following.

Both Bingham and Herschel Bulkley model parameters will be alternatively used to model the gravity induced particle migration in the last part of this paper. Results obtained with the two models will be compared and discussed.

The glass beads used here are SiLibeads® (Type M, Sigmund Linder GmbH). Three diameters are used (2, 5 and 7 mm). The density of the glass beads is 2500 kg/m^3. In order to ensure that these particles behave as rough aggregates, they were first roughened by abrasion and then cleaned by ultrasound in water (Cf. Fig. 2). To prepare the mixtures, the glass beads are slowly added to the carbopol gel and gently stirred manually until a homogenous material is obtained (Cf. Fig. 3).

3.2. Model formwork

The experimental setup used in this study is shown in Fig. 4 [39]. The setup consists of a $20 \times 20 \times 60$ cm container made of transparent Plexiglas, enabling observation of the flow front of the poured fluid. Approximately 6 l of the carbopol containing a 10% volume fraction of glass beads are slowly poured at one side of the form. The pouring speed is roughly 0.1 l/s to avoid any inertia effect [33,42]. We checked that final shape did not depend on pouring rate in this range and we kept the pouring height constant for each test. When the flow stops, image analysis allows for the recording of the final shape of the material. The material is then divided into 6 zones by insertion of metal plates (Cf. Fig. 5). The content of each zone is washed and the volume fraction of glass beads in a given zone is computed from the weight of the beads.

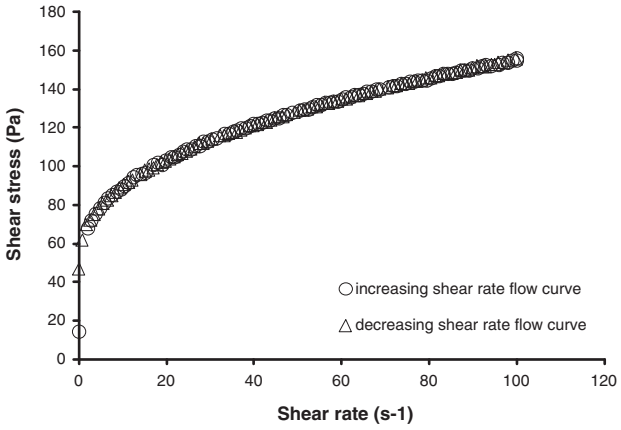

Fig. 1. Flow curve of the carbopol gel.

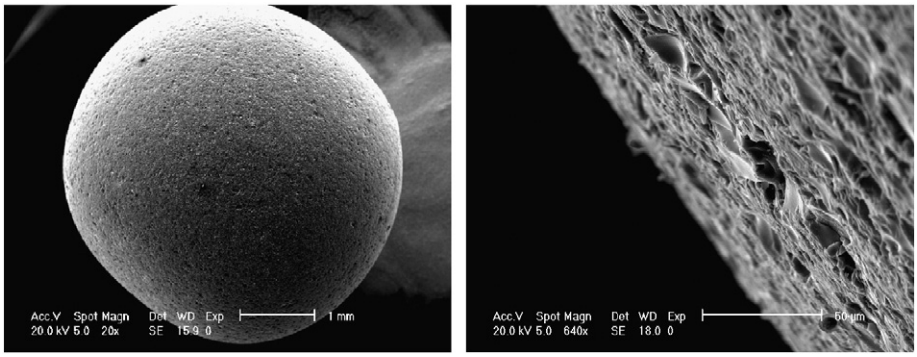

Fig. 2. Surface of the glass beads after abrasion treatment.

4. Numerical simulations

4.1. Prediction of the global flow of the mixture

There exist various numerical techniques allowing for the simulation of the flow of cementitious suspensions [43]. In this paper, a simple and time efficient numerical technique is introduced in order to capture gravity induced particle migration.

Basically, the numerical technique consists in combining the computation of both the global flow of the carbopol and glass beads mixture and, in parallel, the evolution of the local volume fraction of beads. The global flow of the mixture is computed by solving the mass conservation (continuity) equation together with the momentum conservation equations.

In addition, the constitutive behavior of the fluid (carbopol and glass beads mixture) is described with a Bingham material model (see the above section) in which the fluid is at rest when the von Mises stress is below the yield stress and flows according to the plastic viscosity when the von Mises stress is larger than the yield stress. In the numerical formulation, this is approximated with the so-called bi-viscosity model in which the initial viscosity μ_{init} which is used below the yield stress (expressed in terms of the threshold shear rate) is very high as compared to the plastic viscosity μ_p which is used above the yield stress, i.e.:

$$\tau^{ref} = \begin{Bmatrix} \mu_{init}\dot{\gamma}^{ref} & \dot{\gamma}^{ref} < \dot{\gamma}_0 \\ \mu_p\dot{\gamma}^{ref} + \tau_0 = \mu_{app}\dot{\gamma}^{ref} & \dot{\gamma}^{ref} \geq \dot{\gamma}_0 \end{Bmatrix} \tag{6}$$

where $\left(\tau^{ref}\right)^2 = \frac{3}{2}\tau_{ij}\tau_{ij}$ $\tau_{ij} = \sigma_{ij} - \delta_{ij}\sigma_{kk}/3$ *and* $\left(\dot{\gamma}^{ref}\right)^2 = \frac{1}{2}\dot{\gamma}_{ij}\dot{\gamma}_{ij}$

Fig. 3. Homogeneous carbopol gel and glass beads mixture at the end of the mixing phase.

It should be noted here that the threshold value for this implementation is expressed in terms of the threshold strain rate, which relates to yield stress the following way:

$$\dot{\gamma}_0 = \frac{\tau_0}{\mu_{init}}. \tag{7}$$

When the flow is dominated by shear stress τ and shear rate $\dot{\gamma}$, and the initial viscosity is infinitely large, the equations shown above simplify to the Bingham scalar model:

$$\tau = \tau_0 + \mu_p\dot{\gamma} \quad \text{when} \quad \tau \geq \tau_0. \tag{8}$$

The above numerical technique is implemented in the Computational Fluid Dynamics (CFD) code Flow3D®, which is a general purpose software capable of modelling different fluid flow and heat transfer problems. This software allows the user to program subroutines which take into account specific physical phenomena.

4.2. Prediction of the gravity induced particle migration

The evolution of the particle volume fraction is computed by an advection and a settling calculation. The advection makes the volume fraction follow the streamlines of the global flow, while the settling calculation captures the actual settling of the beads. The settling calculation is derived from a mass conservation of the particles:

$$\frac{\partial\phi}{\partial t} + div\left(\phi\,\vec{V}\right) = 0 \tag{9}$$

where ϕ is the local particle volume fraction and $\vec{V}$ is the local particle velocity.

In the settling problem studied here, the local particle velocity is a vertical downward settling velocity V_s, which can be derived from Stokes law (Cf. Section 2.3).

$$V_s = -\frac{ga^2\Delta\rho}{18\mu_0} \tag{10}$$

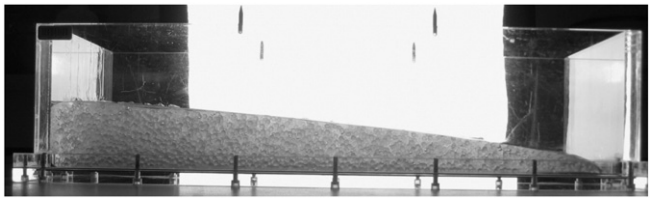

Fig. 4. Model formwork filled with the model material.

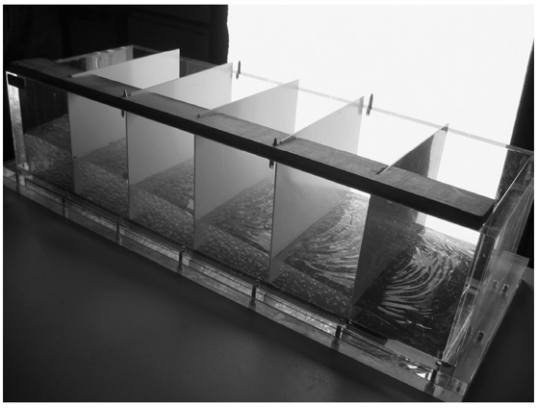

Fig. 5. Zones separation in the model formwork before beads weighting.

where a is the diameter of the glass beads, $\Delta\rho$ is the density difference between the carbopol gel and the glass beads and μ_0 is the local viscosity of the gel around the particle.

As the surrounding fluid is non Newtonian, the question of the nature of the scalar value of this local viscosity arises. The problem is highly three dimensional meaning that several components of the stress tensor may be different from zero. When the components of the stress tensor due to gravity fulfill the von Mises flow criterion, the mixture is flowing. The density difference between the particles and the suspending fluid generates additional stresses in the system. These are combined with the existing stresses at the origin of the global flow of the mixture. Two options can then be considered for the local viscosity of the surrounding fluid. It could either be equal to the apparent viscosity of the material at a shear rate imposed by the flow of the mixture or, as the von Mises criterion is already fulfilled by other components of the stress tensor, to the tangential viscosity (Cf. Fig. 6). In the case of a Bingham fluid model for the suspending fluid, this would be equivalent to considering the plastic viscosity. The gel used in this work can however be described either by a Bingham model for the sake of simplicity or, for a better fit, by a Herschel Bulkley model (Cf. Section 3.1). In the following, we will test the consequences of choosing as an input for the settling numerical simulation the plastic viscosity from the Bingham model, the apparent viscosity from the Herschel Bulkley model or the tangential viscosity from the Herschel Bulkley model (Cf. Fig. 6).

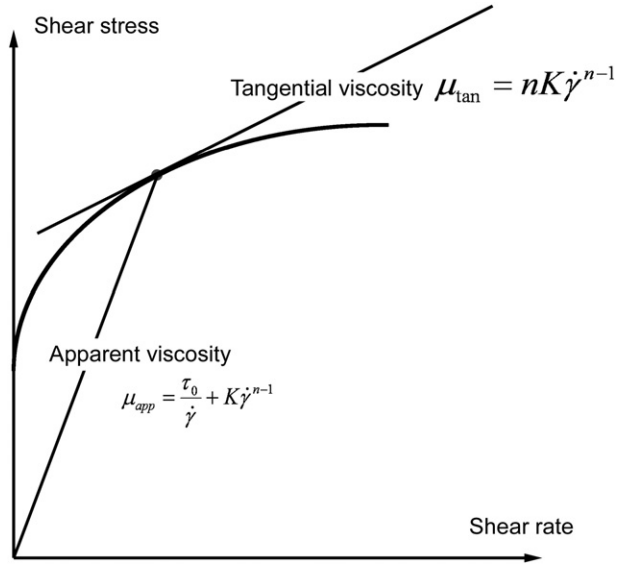

Fig. 6. Apparent and tangential viscosities for a suspending fluid behaving as a Herschel Bulkley material.

Moreover, it can be stressed here once more that, in the simulations carried out in this work, as the influence of the local volume fraction on the local rheology is very low in this range of low volume fractions (see Section 3.1), there is no coupling between the local volume fraction of the glass beads and the rheological behavior of the mixture. Finally, a boundary condition at the bottom of the formwork is implemented to prevent the particles from leaving the computation zone. Additionally, particles are numerically prevented from moving into a cell, in which the dense packing fraction of spheres has already been reached (i.e. 64%).

It can be noted that, in the case of the higher particle volume fractions of real concretes, the above approach would be clearly inappropriate. Particle migration would create a heterogeneous material, in which local viscosity fluctuations due to this migration could play a dominant role in the segregation process. It can be expected that, from a numerical point of view, either advanced discrete methods [44,45] or continuum methods integrating a coupling between local particle volume fraction and drag force [22] would be necessary.

5. Result analysis and discussion

5.1. General description of the experimental results

The measured glass bead volume fractions after the filling of the model formwork are reported in Fig. 7 for the three glass bead diameters. We can first see in this figure that some particle migration is induced by the flow and that the material becomes heterogeneous. This heterogeneity is increasing with the diameter of the glass beads and with the distance from the pouring point. After a flow propagation of 0.6 m, the volume fraction decreases respectively from 10% to 8%, 3% and 1% for the 2, 5 and 7 mm beads. Close to the pouring point, the particle volume fraction is increasing as settling particles gather at the bottom of the model formwork (Cf. Fig. 8).

5.2. Origin of the flow induced particle migration in the model casting

We apply here to our experiments the results from Section 2.6 considering a flow length L of 0.6 m and a flow thickness H of 0.055 m. The initial glass beads concentration ϕ_0 is 10%. The density difference $\Delta\rho$ is 1500 kg/m^3 and the beads diameter a varies between 2 and 7 mm. The flow duration is of the order of 90 s and the flow velocity is therefore of the order of 1 cm/s. The shear rate shall then be of the order of 0.1 s^{-1}. μ_0 may either take the value of the tangent viscosity (around 50 Pa s, Cf. Fig. 1 and Fig. 6) or the apparent viscosity (around 450 Pa s, Cf. Fig. 1 and Fig. 6).

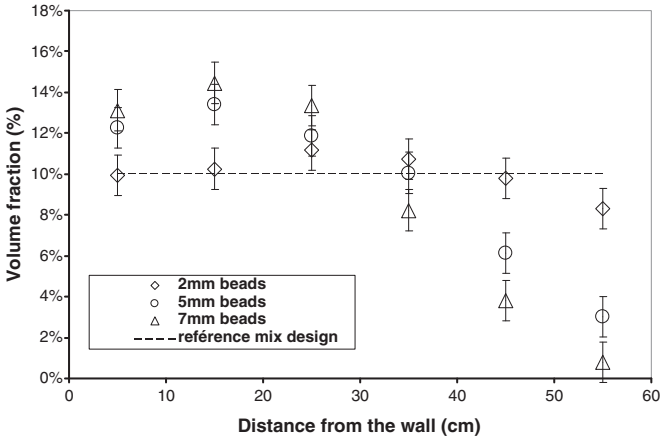

Fig. 7. Measured glass beads volume fractions as a function of the distance in the model formwork.

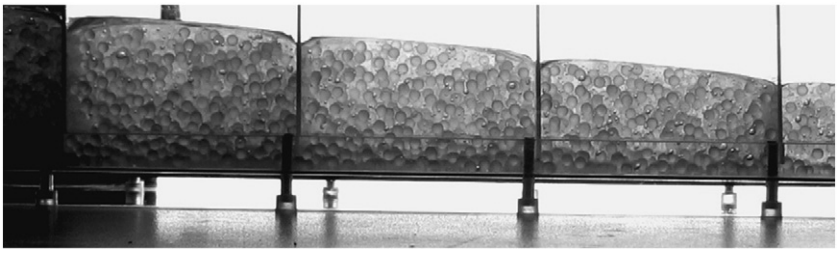

Fig. 8. Glass beads layer at the bottom of the model formwork at the vicinity of the pouring point (7 mm beads).

It can be shown using the relations in Section 2.6 that both shear induced migration and wall effect induced migration are neglectable (Cf. Table 2). This means that, in our experiment as in the casting of fluid concretes, gravity induced heterogeneity dominates all other potential sources of migration. The variations in glass beads volume fraction induced by gravity are then predicted dimensionally to be of the order of 2, 5 and 7% for the glass beads with diameters of 2, 5 and 7 mm if the tangent viscosity is considered and shall respectively be of the order of 0.5, 1 and 2% for the glass beads with diameters of 2, 5 and 7 mm if the apparent viscosity is considered. We can conclude from these estimations that considering the apparent viscosity of the gel results in a strong underestimation of the induced heterogeneity. It can moreover be noted that using the tangential viscosity results in a rather good prediction of the induced migration after 60 cm propagation of the material despite the simplicity of the approaches developed in Section 2.

5.3. Comparison between numerical simulations and experimental results

In Fig. 9, the computed glass beads volume fraction as a function of the distance for three different assumptions on the value of the viscosity of the surrounding carbopol gel is plotted for the 5 mm beads. If we consider for the surrounding fluid the apparent viscosity, numerical simulations underestimate particle migration. If we consider an approximate constant plastic viscosity from the data in Fig. 1, then simulations overestimate the particle migration. It is only when the tangential viscosity is used in the calculation that we obtain a good agreement between simulations and experiments.

This result suggests that the stresses generated by the weight of the mixture fulfill the von Mises flow criterion and are at the origin of the flow. The density difference between the particles and the suspending fluid generates additional stresses in the system. These are combined with the existing stresses at the origin of the global flow of the mixture. As the von Mises criterion is already fulfilled by other components of the stress tensor, these additional stresses only contribute to the viscous dissipation and do not have to overcome the yield stress to generate a relative flow between the particles and the gel. As a consequence, the settling process is the same as the one that would occur in a zero yield stress fluid. The only parameter of interest is therefore the tangential viscosity.

We compare in Fig. 10 the numerical predictions based on the tangential viscosity and the experimental results for the various glass bead sizes. The overall agreement is satisfactory especially if we bear in mind the simplifying assumptions on which the numerical model is built.

6. Relevance of results to real concretes

There exist two main difficulties when expanding the approach proposed here to the case of real concretes.

First, as the volume fraction of coarse aggregates in concrete is far higher than 10% (it is of the order of 40%), the local rheological properties shall depend on the local volume fraction of coarse aggregates. The problem of particle settling becomes therefore a strongly coupled problem as it does not only create heterogeneity in component proportions but also heterogeneities in local rheological properties, which may in turn affect the global flow of the mixture and therefore particle settling (Cf. Section 4.2).

Second, although the behavior of the suspending fluid can be measured in the case of the model material used here, it is not the case for real concrete. It can be expected that the rheological properties to be taken into account shall be between the concrete scale and the mortar scale. Also, the behavior shall be shear thinning as for the carbopol used here. It is however difficult to identify this behavior apart except by using an inverse analysis of a real life flow induced segregation case. As this behavior shall strongly depend on mix design, this type of approach shall only give data for the specific case studied.

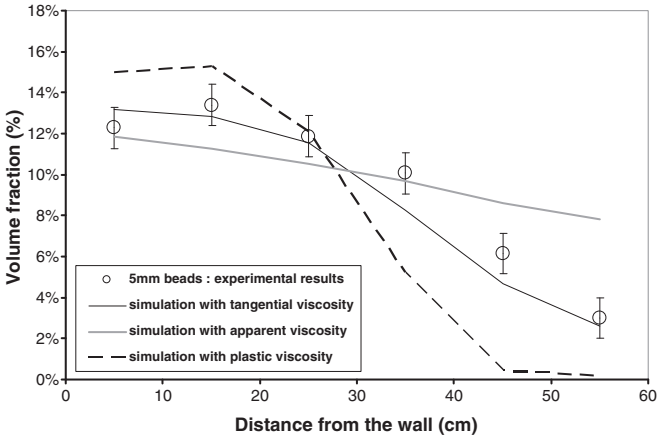

Fig. 9. Glass beads volume fraction as a function of distance for the 5 mm beads. Comparison between experimental results and numerical simulations for various assumptions for the viscosity of the suspending fluid. The yield stress is 40 Pa.

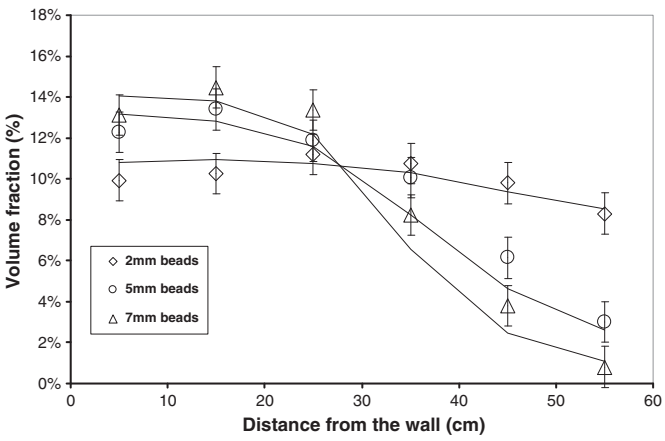

Fig. 10. Glass beads volume fraction as a function of distance for the 2, 5 and 7 mm beads. Comparison between experimental results and numerical simulations considering the tangential viscosity of the surrounding fluid.

We have shown in this paper that the tangential viscosity of the suspending fluid is dictating particle settling. It shall also be the case for real concretes no matter the rheological behavior of the suspending fluid to be considered. The characteristic time of gravity induced segregation (Eq. (4)) then becomes:

$$T_c^{gravity} \cong \frac{H}{V_s} = \frac{18nK\dot{\gamma}^{n-1}H}{g\Delta\rho a^2}. \quad (11)$$

The dimensionless ratio between the duration of the casting process T_f and the above characteristic time gives an idea of the magnitude of the gravity induced segregation for a given process and element to be cast. It scales with the casting velocity as:

$$\frac{T_f}{T_c^{gravity}} \approx V^{-n}. \quad (12)$$

As n shall always be positive, it can therefore be expected that, from a practical point of view, the magnitude of gravity induced segregation shall decrease for fast casting processes. Though intuitively correct, this result has however still to be validated at the scale of concrete. It could indeed be affected by the thixotropic nature of concrete: at high flow rates, the structural break down of the cement paste could lower the tangential viscosity and enhance gravity induced segregation.

7. Conclusions

In this paper, we have described and compared the various physical phenomena which potentially lead to flow induced particle migration in concrete. It was shown that shear induced particle migration and wall effect induced particle migration dominate in the pumping process whereas, in the case of industrial casting of concrete, gravity induced particle migration dominates all other potential sources of heterogeneities induced by flow.

In the second part, we have shown, from comparisons between experiments using model materials, dimensional analysis and numerical simulations, that, from a quantitative point of view, the viscous drag force, which prevents particles from migrating during a casting process, shall neither be computed from the apparent viscosity nor from plastic viscosity of the suspending phase but from its tangential viscosity.

We have moreover shown that it is possible to numerically predict flow induced particle migration during casting of a model material, which was designed to mimic self compacting concrete.

Finally, the transfer of this type of numerical prediction tool to real concrete was discussed.

Acknowledgment

The work is funded by the Danish Agency for Science Technology and Innovation (project 09-065049/FTP: Prediction of flow induced inhomogeneities in self compacting concrete).

References

[1] A.W. Saak, H. Jenning, S. Shah, New methodology for designing self-compacting concrete, ACI Mater. J. 98 (6) (2001) 429–439.
[2] N. Roussel, A theoretical frame to study stability of fresh concrete, Mater. Struct. 39 (2006) 81–91.
[3] M.F. Petrou, B. Wan, F. Galada-Maria, V.G. Kolli, K.A. Harries, Influence of mortar rheology on aggregate settlement, ACI Mater. J. 97 (4) (2000) 479–485.
[4] M.F. Petrou, K.A. Harries, F. Galada-Maria, V.G. Kolli, A unique experimental method for monitoring aggregate settlement in concrete, Cem. Concr. Res. 30 (2000) 809–816.
[5] D. Leighton, A. Acrivos, The shear-induced migration of particles in concentrated suspensions, J. Fluid Mech. 181 (1987) 415–439.
[6] R.J. Phillips, R.C. Armstrong, R.A. Brown, A.L. Graham, J.R. Abbott, A constitutive equation for concentrated suspensions that accounts for shear-induced particle migration, Phys. Fluids 4 (1992) 30–40.
[7] D. Leighton, A. Acrivos, Measurement of shear-induced self-diffusion in concentrated suspensions of spheres, J. Fluid Mech. 177 (1987) 109–131.
[8] A. Acrivos, Bingham award lecture—1994 Shear-induced particle diffusion in concentrated suspensions of noncolloidal particles, J. Rheol. 39 (1995) 813–826.
[9] G. Ovarlez, F. Bertrand, S. Rodts, Local determination of the constitutive law of a dense suspension of noncolloidal particles through magnetic resonance imaging', J. Rheol. 50 (2006) 259–292.
[10] Feys, D., Interactions between rheological properties and pumping of self-compacting concrete, PhD. Uni Ghent (2009).
[11] S. Jacobsen, L. Hauganb, T.A. Hammer, E. Kalogiannidis, Flow conditions of fresh mortar and concrete in different pipes, Cement Concr. Res. 39 (11) (2009) 997–1006.
[12] D. Kaplan, Pompage des bétons, Etudes des recherches des laboratoires des Ponts et Chaussées, Laboratoire Central des Ponts et Chaussées, Paris, 2001 (in French).
[13] Ngo, T.T., Influence de la composition des bétons sur les paramètres de pompage et validation d'un modèle de prévision de la constante visqueuse, PhD. Uni Cergy Pontoise (2009) (In French).
[14] H. Hafid, G. Ovarlez, F. Toussaint, P.H. Jezequel, N. Roussel, Estimating measurement artifacts in concrete rheometers from MRI measurement on model materials, Design, Production and Placement of Self-Consolidating Concrete, Proceedings of SCC2010, Montreal, Canada, , 2010.
[15] Seung Hee Kwon, Seon-Doo Jo, Kyu Park, Jae-Hong Jeong, Seung-Hoon Lee Computational estimation of slip-layer in pipe flow of concrete, proceedings of the 9th International Symposium on High Performance Concrete, 9–11th of August 2011, Rotorua, New Zealand, 2011.
[16] G.Y. Onoda, E.G. Liniger, Random loose packings of uniform spheres and the dilatancy onset, Phys. Rev. Lett. 64 (1990) 2727–2730.
[17] J. Yammine, M. Chaouche, M. Guerinet, M. Moranville, N. Roussel, From ordinary rheology concrete to self compacting concrete: a transition between frictional and hydrodynamic interactions, Cem. Concr. Res. 38 (2008) 890–896.
[18] N. Roussel, A. Lemaître, R.J. Flatt, P. Coussot, Steady state flow of cement suspensions: a micromechanical state of the art, Cement Concr. Res. 40 (2010) 77–84.
[19] A.M. Corbett, R.J. Phillips, R.J. Kauten, K.L. McCarthy, Magnetic resonance imaging of concentration and velocity profiles of pure fluids and solid suspensions in rotating geometries, J. Rheol. 39 (1995) 907–924.
[20] A.L. Graham, S.A. Altobelli, E. Fukushima, L.A. Mondy, T.S. Stephens, Note: NMR imaging of shear-induced diffusion and structure in concentrated suspensions undergoing Couette flow, J. Rheol. 35 (1991) 191–201.
[21] J.R. Abbott, N. Tetlow, A.L. Graham, S.A. Altobelli, E. Fukushima, L.A. Mondy, T.S. Stephens, Experimental observations of particle migration in concentrated suspensions: Couette flow, J. Rheol. 35 (1991) 773–795.
[22] L. Shen, L. Struble, D. Lange, Modeling dynamic segregation of self-consolidating concrete, ACI Mater. J. 106 (4) (2009) 375–380.
[23] D. Lowke, T. Kränkel, C. Gehlen, P. Shiessl, Effect of cement on super plasticizer adsorption, Yield stress, Thixotropy and Segregation resistance, in: K. Khayat, D. Feys (Eds.), Proceedings of SCC2010, Montreal, Canada, Springer, 2010, pp. 91–102.
[24] N. Roussel, A thixotropy model for fresh fluid concretes: theory, validation and applications, Cement Concr. Res 36 (10) (2006) 1797–1806.
[25] N. Roussel, Steady and transient flow behaviour of fresh cement pastes, Cement Concr. Res. 35 (9) (2005) 1656–1664.
[26] NF EN 1992-1-1 Eurocode 2 (2005).
[27] T. Sedran, F. de Larrard, Optimization of self compacting concrete thanks to packing model, RILEM Symposium on Self Compacting Concrete, September 1999, pp. 321–332, Stockholm, 13–15.
[28] N. Roussel, T.L.H. Nguyen, O. Yazoghli, P. Coussot, Passing ability of fresh concrete: a probabilistic approach, Cement Concr. Res. 39 (2009) 227–232.
[29] F. Chevoir, F. Gaulard, N. Roussel, Flow and jamming of granular mixtures through obstacles, Europhysics Lett. 79 (2007) 14001.
[30] N. Roussel, T.l.h. Nguyen, P. Coussot, General probabilistic approach of filtration process, Phys. Rev. Lett. 98 (11) (2007) 114502.
[31] Tam, C.T., Shein, A.M.M., Ong, K.C.G., Chay, C.Y., Modified J-ring approach for assessing passing ability of SCC, proceedings of SCC 2005, published by Hanley Wood, 2005.
[32] I.Y.T. Ng, H.H.C. Wong, A.K.H. Kwan, Passing ability and segregation stability of self-consolidating concrete with different aggregate proportions, Mag. Concr Res. 58 (6) (2006) 447–457.
[33] T.L.H. Nguyen, N. Roussel, P. Coussot, Correlation between L-box test and rheological parameters of an homogeneous yield stress fluid, Cement Concr. Res. 36 (10) (2006) 1789–1796.
[34] F. de Larrard, Concrete Mixture Proportioning, E & FN Spon, London, 1999.
[35] O. Wallevik, Rheology — a scientific approach to develop self-compacting concrete, Proceedings of the 3rd international RILEM Symposium on Self-Compacting Concrete, Reykjavik, Iceland, 2003, pp. 23–31, (RILEM PRO33, 2003).
[36] N. Roussel, The LCPC BOX: a cheap and simple technique for yield stress measurements of SCC, Mater. Struct. 40 (9) (2007) 889–896.
[37] C.F. Ferraris, L.E. Brower (Eds.), Comparison of concrete rheometers: international tests at LCPC (Nantes, France) in October, 2000, National Institute of Standards and Technology Interagency Report (NISTIR) 6819., , 2001.
[38] C.F. Ferraris, L.E. Brower (Eds.), Comparison of concrete rheometers: international tests at MB (Cleveland OH, USA) in May, 2003, National Institute of Standards and Technology Interagency Report (NISTIR) 7154., , 2004.
[39] Nguyen, T.L.H. (2007) « Outils pour la modélisation de la mise en œuvre des bétons », Doctoral thesis, Laboratoire central des Ponts et chaussées, ENPC p.122 (in French).
[40] X. Chateau, G. Ovarlez, K.L. Trung, Homogenization approach to the behavior of suspensions of noncolloidal particles in yield stress fluids, J. Rheol. 52 (2008) 489–506.

[41] F. Mahaut, S. Mokeddem, X. Chateau, N. Roussel, G. Ovarlez, Effect of coarse particle volume fraction on the yield stress and thixotropy of cementitious materials, Cem. Concr. Res. 38 (2008) 1276–1285.
[42] N. Roussel, Correlation between yield stress and slump: comparison between numerical simulations and concrete rheometers results, Mater. Struct. 39 (4) (2006) 501–509.
[43] N. Roussel, M.R. Geiker, F. Dufour, L.N. Thrane, P. Szabo, Computational modeling of concrete flow: general overview, Cement Concr. Res. 37 (9) (2007) 1298–1307.
[44] N.S. Martys, Study of a dissipative particle dynamics based approach for modeling suspensions, J. Rheol. 49 (2) (2005) 401–424.
[45] N. Martys, C.F. Ferraris, Simulation of SCC flow, Proc. 1st North American Conf. on the design and use of Self-Consolidating Concrete, Chicago, IL, 2002, pp. 27–30.